



This is a repository copy of *Torsional oscillations within a magnetic pore in the solar photosphere*.

White Rose Research Online URL for this paper:
<https://eprints.whiterose.ac.uk/174330/>

Version: Accepted Version

Article:

Stangalini, M., Erdélyi, R., Boocock, C. et al. (5 more authors) (2021) Torsional oscillations within a magnetic pore in the solar photosphere. *Nature Astronomy*, 5 (7). pp. 691-696. ISSN 2397-3366

<https://doi.org/10.1038/s41550-021-01354-8>

This is a post-peer-review, pre-copyedit version of an article published in *Nature Astronomy*. The final authenticated version is available online at:
<https://doi.org/10.1038/s41550-021-01354-8>

Reuse

Items deposited in White Rose Research Online are protected by copyright, with all rights reserved unless indicated otherwise. They may be downloaded and/or printed for private study, or other acts as permitted by national copyright laws. The publisher or other rights holders may allow further reproduction and re-use of the full text version. This is indicated by the licence information on the White Rose Research Online record for the item.

Takedown

If you consider content in White Rose Research Online to be in breach of UK law, please notify us by emailing eprints@whiterose.ac.uk including the URL of the record and the reason for the withdrawal request.



eprints@whiterose.ac.uk
<https://eprints.whiterose.ac.uk/>

Torsional Oscillations in a Magnetic Pore in the Solar Photosphere

Alfvén waves have proven important in a range of physical systems (e.g., stars, planetary atmospheres, tokamaks) due to their ability to transport non-thermal energy over long distances in a magnetised plasma. This property is of specific interest in solar physics where the extreme heating of the solar atmosphere remains unexplained. **In an inhomogeneous plasma like a flux tube in the solar atmosphere, they exist in the form of incompressible torsional perturbations, which have magnetic tension as their sole restoring force.** Despite several claims in the upper layers of the Sun's atmosphere their direct signature, torsional oscillations of magnetic iso-contours, is yet to be observed. This is because detecting signatures of torsional oscillations in a magnetic structure with high-enough sensitivity remains a challenge. Here, we report the detection of anti-phase **incompressible** torsional oscillations ~~of the circular polarisation (a proxy for the line-of-sight magnetic field)~~ measured in a magnetic pore in the photosphere of the Sun. Supporting state-of-the-art simulations **suggest a possible** excitation mechanism of these waves.

The observational confirmation of the presence of torsional waves in photospheric magnetic structures could have a wide impact on our understanding of the energy transport in the solar atmosphere, especially if such signatures will be ubiquitously detected in even smaller structures with the forthcoming next generation of solar telescopes.

~~The search for torsional oscillations in magnetic structures in the lower solar atmosphere was the main focus of a number of studies in recent years. Most of such studies were focused on the identification of Alfvén waves, incompressible plasma perturbations which have magnetic tension as their sole restoring force.~~

The existence of Alfvén waves was predicted theoretically more than 70 years ago¹ and they were immediately recognized for their potential impact in many research areas, including neutrino physics², the heating of the solar upper atmosphere - the corona - to million-degree temperatures^{3,4}, proto-stellar disks⁵, the physics of the interstellar medium⁶, particle acceleration around supermassive black holes⁷, and nuclear fusion research, where these magnetic waves have been proposed as a possible effective heating mechanism in tokamaks^{8,9}.

One of the fundamental major applications in plasma physics is that torsional waves play a key role in the transportation and dissipation of energy potentially leading to heating. Examples where these properties could be important include both laboratory and space plasmas such as e.g. the intergalactic medium, plasma fusion reactors, or the solar atmosphere from the chromosphere to the corona. In solar magnetic flux tubes, these waves manifest as either axisymmetric or anti-symmetric torsional perturbations¹⁰ (Torsional Alfvén waves; hereafter TAWs). A number of studies have presented a range of indirect confirmations of Alfvén wave manifestation¹¹ over the past decades including counter-flowing velocities at opposite sides of solar jets and perturbations to spectral line widths. These earlier studies have been limited mostly to the upper solar atmosphere^{12,13} and solar wind¹⁴, ~~meaning despite their apparent importance, meaning that no observation of torsional motion that could be linked to TAWs¹⁵ has been directly detected in the photosphere.~~ Therefore, Alfvén waves remain the most elusive, yet physically intriguing, class of magnetohydrodynamic (MHD) waves that are still waiting to be fully understood despite decades of research. ~~After their discovery, Alfvén waves were immediately recognized for their potential impact in many research areas, including neutrino physics², the heating of the solar upper atmosphere - the corona - to million-degree temperatures^{3,4}, proto-stellar disks⁵, the physics of the interstellar medium⁶, particle acceleration around supermassive black holes⁷, and nuclear fusion research, where these magnetic waves have been proposed as a possible effective heating mechanism in tokamaks^{8,9}.~~ So far, despite the many suggestions of the presence of Alfvén waves in the upper layers of the solar atmosphere^{12,13} and in the solar wind¹⁴, no observation of torsional motion that could be linked to TAWs¹⁵ has been reported in the photosphere.

One of the fundamental major applications in plasma physics is that torsional waves play a key role in the energy transportation, heating and energy dissipation. Examples include both laboratory and space plasmas such as the solar atmosphere from the chromosphere to the corona, the intergalactic medium, or plasma fusion reactors. In this article, we present the detection of non-axisymmetric torsional oscillations in a compact photospheric magnetic structure, made possible by high-resolution observations acquired by the IBIS¹⁶ 2D

spectropolarimeter at the Dunn Solar Telescope (DST, New Mexico, USA). We interpret these oscillations to be direct signatures of TAWs in the solar photosphere.

Spectropolarimetry has long been a standard method used to infer magnetic fields in the Sun and other stars; however, the spatial, temporal, and spectral resolutions we can now achieve with observations of our nearest star means the polarimetric footprint left by the magnetic field in the Sun's photospheric plasma can now be exploited to map and study its magnetic structures and their associated dynamics in fine detail. Specifically, the high temporal and spatial resolutions (scales close to 120 km on the surface of the Sun can be sampled a few times every minute) achieved by modern 2D solar spectro-polarimetric imagers such as IBIS, are perfect for studying the fine-structure and rapid dynamical behaviour of photospheric magnetic structures such as pores. The instantaneous circular polarization map of the light emerging from the pore studied here in the magnetically sensitive $Fe\ I\ 617.3\text{ nm}$ spectral line is plotted in Fig. 1 (panel a). This represents a direct indicator of the vertical magnetic field of the structure at this time. The ~ 69 min duration and 52 s temporal resolution of the IBIS dataset studied here allow us to investigate the evolution of the entire magnetic structure and, specifically, to trace torsional magnetic oscillations, perpendicular to the line-of-sight, through time. To achieve this aim, we initially transform the temporal sequence of circular polarization maps into polar coordinates (see Fig. S1 for an example). The approximate position of the centres of the two magnetic lobes (marked by the two red crosses in Fig. 1 panel a) are employed as the radial origins of the structures. Over-plotted on Fig. 1 (panel a) are the streamlines of the torsional oscillations indicating its $m = 1$ dipolar nature. The measured angular shifts of both lobes, as a function of time, are shown in Fig. 1 (panel b), where it is simple to recognize a periodic angular displacement in both sides of the pore. It is worth noting that the torsional oscillations of the two lobes are out of phase. The thickness of the curves indicates the 3σ error associated with the measures (see Appendix for more details).

A series of supporting 3D MHD simulations were performed using Lare3d¹⁷ to demonstrate a possible formation mechanism for $m = 1$ TAWs in the lower solar atmosphere. Similar to¹⁸, these simulations show the excitation of TAWs as a result of coupling with kink oscillations. Lare3d is a Lagrangian remap code that solves the resistive MHD equations over a 3D staggered grid¹⁹. A high-density, vertically stratified, divergent, flux tube was placed at the centre of the domain, representing the magnetic pore, and linear Alfvén waves are then driven from the lower boundary, modeling the observed photospheric surface. It is found that the investigated magnetic flux tube exhibits structural non-axisymmetric torsional oscillations, manifesting as periodic non-axisymmetric rotation of the two lobes composing the magnetic structure. The rotation of the magnetic fields at a height of 500 km above the photosphere is shown in Fig. 1 (panel c). These supplementary, state-of-the-art numerical simulations show underpinning evidence for the presence of anti-symmetric magnetic field and plasma velocity oscillations that, similar to¹⁸, are consistent with $m = 1$ torsional Alfvén waves within a model solar photospheric magnetic structure (a cartoon depiction is plotted in Fig. 1 panel d). The two counter-rotating oscillations in the velocity and magnetic fields are readily identifiable in Figs. S6 and S7. These supporting visualisations were developed to highlight the dynamics of these oscillations, with movies being presented in the Supplementary Material. At the density inhomogeneity of the flux tube, transverse wave modes are coupled to the $m = 1$ torsional Alfvén mode similar to the coupling of kink modes to the $m = 1$ Alfvén mode described in²⁰. The typical result shown here **suggests a formation mechanism** of two counter-rotating oscillations either side of the flux tube.

The velocity power spectra of the torsional oscillations in the observed pore are shown in Fig. 2 (panel a). In the same plot, we highlight the confidence levels as estimated from a bootstrapping randomization test making use of 1000 runs (see Appendix for more details). Several harmonics with confidence levels larger than 95% are seen in the spectra of the two lobes. In Fig. 2 (panel b), we show the scaling law of the peaks found in the right lobe, as obtained from a multi-Gaussian fit to the spectrum. The power spectra of the torsional oscillations of the two lobes exhibit several peaks consistent with harmonics of standing oscillations. **Similar to what is reported widely in the literature for resonant oscillations of the flux tubes at various heights in the solar atmosphere²¹⁻²³, some of the harmonics are characterized by an intermittent and non-stationary behaviour.**

We note that the presence of harmonics rules out the possibility that the observed torsional oscillations might be the results of noise or seeing effects. The fit to the data yields fundamental frequency $\nu_f = 0.65 \pm 0.02\text{ mHz}$, corresponding to a period of about 25 min.

Next, in order to provide a first insight into the associated Alfvén wave energy flux, we make use of the following relation,

$$E = \rho v^2 c_A, \quad (1)$$

where ρ is the mass density, v the velocity of oscillation, and c_A the Alfvén wave phase speed. Substituting the average magnetic field obtained from the COG method²⁴ in the annular regions, and the average values of the density as estimated from spectropolarimetric inversions (see Appendix), into this equation we have an estimate of the energy content of the two lobes. Given the measured value of the root mean square velocity amplitude of the torsional oscillations ($v_{\text{left}} \sim 0.4 \text{ km s}^{-1}$ and $v_{\text{right}} \sim 0.3 \text{ km s}^{-1}$), the estimated energy flux is $E_{\text{left}} = 135 \pm 85 \text{ kW/m}^2$ and $E_{\text{right}} = 140 \pm 80 \text{ kW/m}^2$ for the two lobes, respectively. These values are in excess of the required energy flux needed to heat the active region chromosphere ($\sim 20 \text{ kW m}^{-2}$) and corona ($\sim 10 \text{ kW m}^{-2}$)²⁵. This implies that, in the upper limit regime (lower error bound) $\sim 50\%$ of the total estimated energy would need to be dissipated to heat the active region chromosphere and corona. This energy content is therefore quite large with respect to the required value, however, it is worth noting that not all the energy contained in the waves may be transported to the upper atmosphere or converted to thermal energy at those heights. We note that the above estimates of the energy flux are only applicable to a single, fixed frequency. If, instead of a single frequency, a wide spectrum is considered, commensurately, more heating can be provided as is shown in¹⁹.

Obtaining long-duration excellent quality **spectropolarimetric** data, like those used in this work, is generally hampered by the large variability of daytime seeing conditions. For this reason, it is difficult to judge how ubiquitous these torsional motions can be, and whether they are the key to a steady heating mechanism of the chromosphere and corona.

Further, we would also like to comment on some alternative interpretation **of the results**. It has been shown²⁶ that kink waves can also generate velocity fields that are spatially and temporally varying sums of both transverse and rotational motion. With other words, such bulk transverse motions in flux tubes also have omnipresent rotational motions that actually may appear similar to those in our observations and simulations that we interpret as $m=1$ TAW. While other authors have interpreted a similar behavior as a coupling and excitation mechanism of TAWs, we find this is an interesting alternative to be considered. However, our simulations show incompressible torsional oscillations (see the supplementary material), hence providing support for our TAW interpretation.

Our simulations suggest a possible excitation mechanism of the torsional oscillations in the lower solar atmosphere, which may constitute an effective mechanism for extracting energy from the solar photosphere itself.

Regarding the possible damping mechanisms of torsional Alfvén waves, one such process expected to occur in the solar plasma is phase mixing^{27,28}. In flux tube geometry, this requires a varying background Alfvén speed in the radial direction, i.e., perpendicular to the tube axis. Since the magnetic field strength does indeed change as a function of radius in the pore, there will also be a varying Alfvén speed, enabling the necessary conditions for phase mixing to take place. This process may cause the torsional velocity perturbations in neighboring streamlines to go out-of-phase with height, allowing the possibility of the development of Kelvin-Helmholtz instability²⁷, thus generating smaller length scales at which plasma heating becomes more efficient²⁸. Higher in the atmosphere, for example, in the corona, the resultant sub-resolution incoherent motions due to these processes could contribute significantly to observed non-thermal line widths, which are known to be much greater in magnitude than actual resolved Doppler velocities²⁹.

Finally, we would like to stress that our numerical simulations indicate that when a (vertical) magnetic flux tube is driven at the bottom with a linearly polarized Alfvén wave with frequencies similar to **the local Alfvén frequency** or below, then the generated $m=1$ torsional Alfvén wave is excited. At the density inhomogeneity within the umbra of the flux tube transverse wave modes are coupled to the $m=1$ torsional Alfvén mode through e.g. resonant damping similar to the coupling of kink modes to the $m=1$ Alfvén mode described in²⁰. A typical result of such numerical modelling shown here demonstrates the formation of two counter-rotating oscillations either side of the flux tube. These supplementary numerical simulations are not in any way contrived. On the contrary, the described process of $m=1$ TAW mode excitation is a natural process and is expected to be ubiquitous in the solar photosphere.

References

1. Alfvén, H. Existence of Electromagnetic-Hydrodynamic Waves. *Nature* **150**, 405–406 (1942).
2. Bahcall, J. N. & Bethe, H. A. Solution of the solar-neutrino problem. *Phys. Rev. Lett.* **65**, 2233–2235 (1990).
3. Erdélyi, R. & Fedun, V. Are There Alfvén Waves in the Solar Atmosphere? *Science* **318**, 1572– (2007).
4. Liu, J., Nelson, C. J., Snow, B., Wang, Y. & Erdélyi, R. Evidence of ubiquitous Alfvén pulses transporting energy from the photosphere to the upper chromosphere. *Nature Communications* **10**, 3504 (2019).
5. Vasconcelos, M. J., Jatenco-Pereira, V. & Opher, R. Alfvénic Heating of Protostellar Accretion Disks. *ApJ* **534**, 967–975 (2000).
6. McKee, C. F. & Zweibel, E. G. Alfvén Waves in Interstellar Gasdynamics. *The Astrophysical Journal* **440**, 686 (1995).
7. Ebisuzaki, T. & Tajima, T. Astrophysical ZeV acceleration in the relativistic jet from an accreting supermassive blackhole. *Astroparticle Physics* **56**, 9–15 (2014).
8. Hasegawa, A. & Chen, L. Kinetic processes in plasma heating by resonant mode conversion of Alfvén wave. *The Physics of Fluids* **19**, 1924–1934 (1976).
9. Chen, L. & Hasegawa, A. Plasma heating by spatial resonance of Alfvén wave. *The Physics of Fluids* **17**, 1399–1403 (1974).
10. Spruit, H. C. Propagation speeds and acoustic damping of waves in magnetic flux tubes. *Solar Physics* **75**, 3–17 (1982).
11. Mathioudakis, M., Jess, D. B. & Erdélyi, R. Alfvén Waves in the Solar Atmosphere. From Theory to Observations. *Space Sci. Rev.* **175**, 1–27 (2013).
12. Jess, D. B., Mathioudakis, M., Erdélyi, R., Crockett, P. J., Keenan, F. P., Christian, D. J., Alfvén Waves in the Lower Solar Atmosphere. *Science* **323**, 1582– (2009).
13. Kohutova, P., Verwichte, E. & Froment, C. First direct observation of a torsional Alfvén oscillation at coronal heights. *A&A* **633**, L6 (2020).
14. Velli, M. & Pruneti, F. Alfvén waves in the solar corona and solar wind. *Plasma Phys. Control. Fusion* **39**, B317–B324 (1997).
15. Doorselaere, T. V., Nakariakov, V. M. & Verwichte, E. Detection of Waves in the Solar Corona: Kink or Alfvén? *ApJ* **676**, L73 (2008).
16. Cavallini, F. IBIS: A New Post-Focus Instrument for Solar Imaging Spectroscopy. *Sol. Phys.* **236**, 415–439 (2006).
17. Arber, T. D., Longbottom, A. W., Gerrard, C. L. & Milne, A. M. A Staggered Grid, Lagrangian–Eulerian Remap Code for 3-D MHD Simulations. *Journal of Computational Physics* **171**, 151–181 (2001).
18. Pascoe, D. J., Wright, A. N. & De Moortel, I. Coupled Alfvén and Kink Oscillations in Coronal Loops. *The Astrophysical Journal* **711**, 990–996 (2010).
19. Tsiklauri, D. & Nakariakov, V. M. Wide-spectrum slow magnetoacoustic waves in coronal loops. *Astronomy and Astrophysics* **379**, 1106–1112 (2001).
20. Tsiklauri, D. A mechanism for parallel electric field generation in the MHD limit: possible implications for the coronal heating problem in the two stage mechanism. *A&A* **455**, 1073–1080 (2006).
21. Roberts, B., Edwin, P. M. & Benz, A. O. On coronal oscillations. *The Astrophysical Journal* **279**, 857–865 (1984).
22. Nakariakov, V. M., Pascoe, D. J. & Arber, T. D. Short Quasi-Periodic MHD Waves in Coronal Structures. *ßr* **121**, 115–125 (2005).
23. Dorotovič, I., Erdélyi, R., Freij, N., Karlovský, V. & Márquez, I. Standing sausage waves in photospheric magnetic waveguides. *Astronomy and Astrophysics* **563**, A12 (2014).
24. Rees, D. E. & Semel, M. D. Line formation in an unresolved magnetic element - A test of the centre of gravity method. *Astronomy and Astrophysics* **74**, 1–5 (1979).
25. Withbroe, G. L. & Noyes, R. W. Mass and energy flow in the solar chromosphere and corona. *Ann. Rev. Astron. Astrophys.* **15**, 363–387 (1977).
26. Goossens, M., Soler, R., Terradas, J., Van Doorselaere, T. & Verth, G. The transverse and rotational motions of magnetohydrodynamic kink waves in the solar atmosphere. *The Astrophysical Journal* **788**, 9 (2014).
27. Browning, P. K. & Priest, E. R. Kelvin-Helmholtz instability of a phased-mixed Alfvén wave. *Astronomy and Astrophysics* **131**, 283–290 (1984).
28. Soler, R., Terradas, J., Oliver, R., Ballester, J. L. & Goossens, M. Kelvin-Helmholtz Instability in Coronal Magnetic Flux Tubes due to Azimuthal Shear Flows. *The Astrophysical Journal* **712**, 875–882 (2010).
29. McIntosh, S. W. & Pontieu, B. D. ESTIMATING THE “DARK” ENERGY CONTENT OF THE SOLAR CORONA. *ApJ* **761**, 138 (2012).
30. van Noort, M., Rouppe van der Voort, L. & Löfdahl, M. ~G. Solar Image Restoration By Use Of Multi-frame Blind Deconvolution With Multiple Objects And Phase Diversity. *Sol. Phys.* **228**, 191–215 (2005).
31. Reardon, K. P. & Cavallini, F. Characterization of Fabry-Perot interferometers and multi-etalon transmission profiles. The IBIS instrumental profile. *A&A* **481**, 897–912 (2008).
32. Fisher, R. a. *The Design Of Experiments.* (1935).
33. Linnell Nemec, A. F. & Nemec, J. M. A test of significance for periods derived using phase-dispersion-minimization techniques. *The Astronomical Journal* **90**, 2317–2320 (1985).
34. O’Shea, E., Banerjee, D., Doyle, J. ~G., Fleck, B. & Murtagh, F. Active region oscillations. *ApJ* **368**, 1095–1107 (2001).
35. Vernazza, J. E., Avrett, E. H. & Loeser, R. Structure of the solar chromosphere. III - Models of the EUV brightness components of the quiet-sun. *The Astrophysical Journal Supplement Series* **45**, 635–725 (1981).

Acknowledgements

Will be included at a later stage when double-blind peer review process ends

Author contributions

Will be included at a later stage when double-blind peer review process ends

Author information

Will be included at a later stage when double-blind peer review process ends

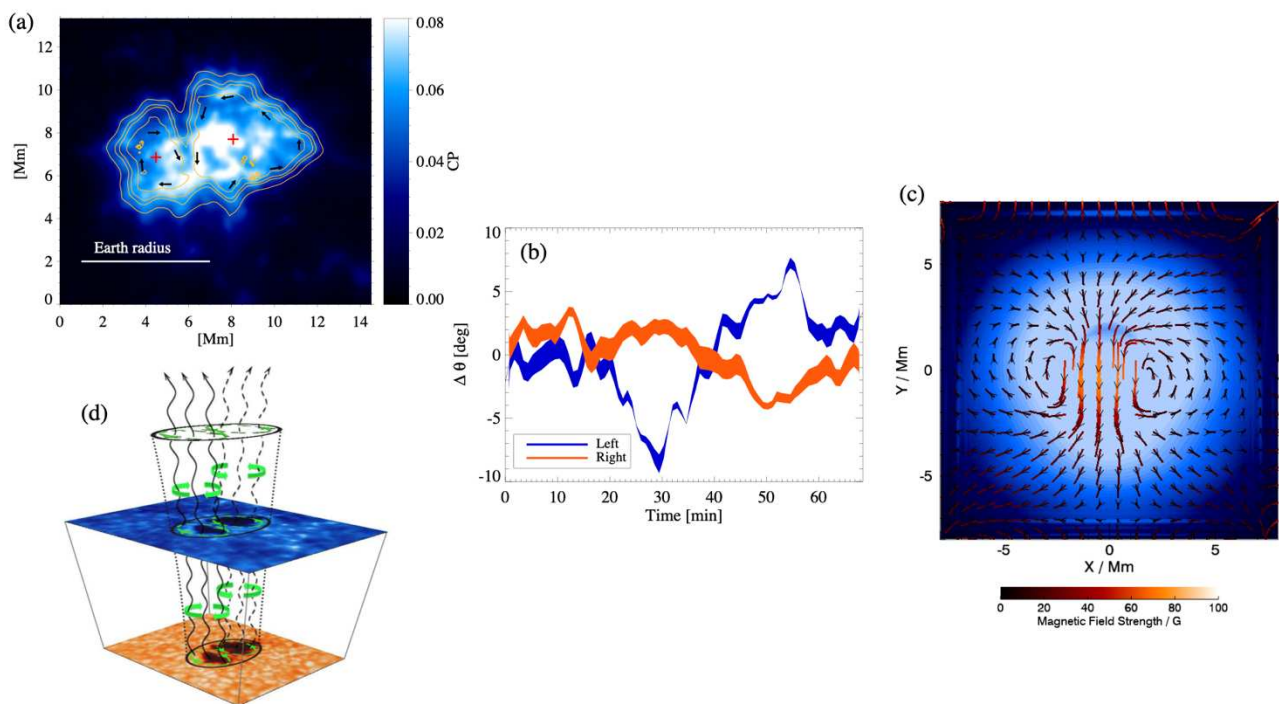


Figure 1. Detection of torsional oscillations in a compact magnetic structure in the solar photosphere. (a) Circular Polarization map of the magnetic pore observed by IBIS@DST. (b) Measured angular rotation oscillations of the two lobes of the magnetic pore, as obtained from a cross-correlation tracking analysis at the edges of the flux tube. (c) Supplementary numerical simulation showing horizontal magnetic field perturbations for the $m=1$ torsional Alfvén wave over a contour of the magnetic field strength. (d) Cartoon depicting the $m=1$ anti-symmetric torsional Alfvén oscillations in solar context.

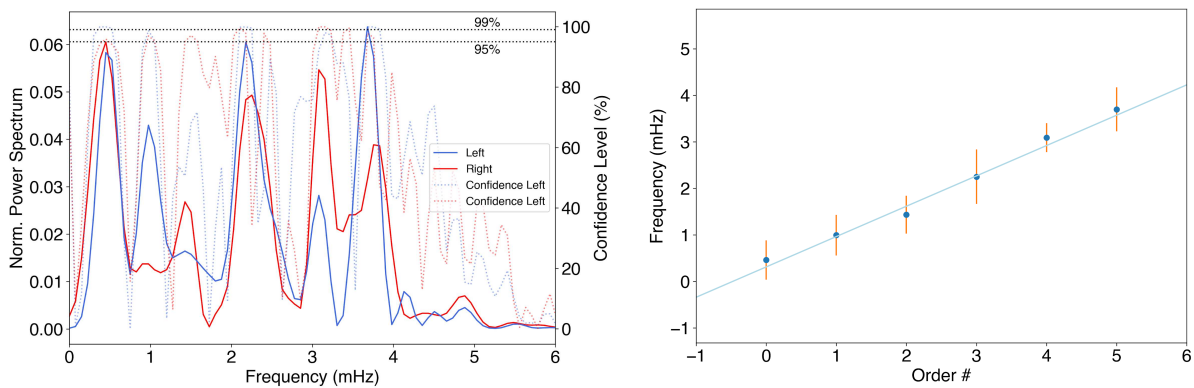


Figure 2. Power spectrum of the torsional oscillations and harmonics.

Power spectrum of the torsional velocity of the two lobes (left) showing the presence of several peaks, scaling as harmonics (right, see Supplementary Material for more details). The average of the velocity time series is subtracted and the time series themselves are normalized by their standard deviation before estimating the power spectrum. On the same plot we also show the confidence levels as obtained by a bootstrapping randomization test with 1000 runs (horizontal dotted lines).

List of Online movies:

TubeDrive500km.mp4: A video showing partial fluid streamlines perpendicular to the flux tube at a height of 500 km above the photosphere. The strength of the streamlines is shown by their length and colour as indicated by the colour bar. The streamlines are overlaid on a counter of the density clearly showing the position of the flux tube. The video clearly shows the formation of torsional motions at the tube boundary.

TubeDrive1mm.mp4: A video showing partial fluid streamlines perpendicular to the flux tube at a height of 1 Mm above the photosphere. The strength of the streamlines is shown by their length and colour as indicated by the colour bar. The streamlines are overlaid on a counter of the density clearly showing the position of the flux tube. The video clearly shows the formation of torsional motions at the tube boundary.

TubeDrive2mm.mp4: A video showing partial fluid streamlines perpendicular to the flux tube at a height of 2 Mm above the photosphere. The strength of the streamlines is shown by their length and colour as indicated by the colour bar. The streamlines are overlaid on a counter of the density clearly showing the position of the flux tube. The video clearly shows the formation of torsional motions at the tube boundary.

B_TubeDrive500km.mp4: A video showing the field lines of the magnetic perturbation perpendicular to the flux tube at a height of 500 km above the photosphere. The strength of the field lines is shown by their length and colour as indicated by the colour bar. The field lines are overlaid on a counter of the density clearly showing the position of the flux tube. The video clearly shows the formation of torsional magnetic perturbations at the tube boundary.

B_TubeDrive1mm.mp4: A video showing the field lines of the magnetic perturbation perpendicular to the flux tube at a height of 1 Mm above the photosphere. The strength of the field lines is shown by their length and colour as indicated by the colour bar. The field lines are overlaid on a counter of the density clearly showing the position of the flux tube. The video clearly shows the formation of torsional magnetic perturbations at the tube boundary.

B_TubeDrive2mm.mp4: A video showing the field lines of the magnetic perturbation perpendicular to the flux tube at a height of 2 Mm above the photosphere. The strength of the field lines is shown by their length and colour as indicated by the colour bar. The field lines are overlaid on a counter of the density clearly showing the position of the flux tube. The video clearly shows the formation of torsional magnetic perturbations at the tube boundary.

Methods

The data of this study were acquired on 15th October 2008, commencing at 16:30 UT, with the IBIS instrument at the DST. The observations combined high-spectral resolution with short exposure times and a large field-of-view. The region presented here is AR 11005 which manifested as a small pore with a light bridge at a latitude [25.2° N, 10.0° W]. This dataset consists of 80 sequences of measurements, each containing a 21-point-scan of the Fe I 617.3 nm line with full Stokes profiles. The difference in wavelength between the sampled points of the Fe I line was 0.002 nm and the exposure time for each image was set to 80 ms, and each spectral scan took approximately 52 s to complete. These narrow-band data collected by the 1024×1024 pixel CCD camera were binned into 2 × 2 pixels giving a final pixel scale of these 512 × 512 images as 0.167 arcsec. For each narrow-band image, we also acquired a broad-band white light (WL; 621.3 ± 5 nm) counterpart, imaging the same field-of-view. The pixel scale of the 1024 × 1024 WL image was set at 0.083 arcsec and the exposure time was 80 ms. Each WL exposure was precisely aligned to the exposures of the narrow-band images through the shared use of a single shutter. Simultaneous WL images are used as a reference frame for the restoration of spectral images with the Multi-Frame Blind Deconvolution³⁰ (MFBD).

The reduction pipeline takes care of normal calibration processes (dark frames, flat fielding, etc.) and also corrects for blue-shift effects³¹ and instrumental polarization. Residual cross-talks are reduced down to the noise level of the images, thus their effects can be safely neglected. In order to limit thermal effects, the local continuum I_c is chosen to normalise the spectral profiles. The photospheric Fe I data were used to estimate the total circular polarization (CP). This yields a map of CP for every frame in the data sequence. We remark that CP signals can be attributed to the line-of-sight (LOS) magnetic field. Before analysing the torsional oscillations, the residual tip-tilt motion was removed by means of a FFT cross-correlation technique with subpixel accuracy.

The analysis of the calibrated data consisted of the simple strategy of plotting the circular polarization maps in polar coordinates (see Fig. S1). At each temporal step, the two lobes composing the magnetic structure are mapped into polar coordinates with origins at the approximate centres indicated by the red crosses of Fig. 1 (main text). The exact position of the centre of each lobe is chosen as the one maximizing the amplitude of the observed oscillations. In the CP polar maps a band enclosing the boundary of the magnetic structure is chosen. After that, an FFT (Fast Fourier Transform) correlation is used to estimate the torsional displacement of the flux tube which manifests as a horizontal shift of this part of the polar maps in consecutive temporal steps. It is worth noting here that the estimation of the angular displacement of the two lobes of the magnetic structure simply reduces to the tracking of the boundaries of the structure itself. In Fig. 1 (main text) the angular oscillations of the two regions of the magnetic structure are shown as a function of time. In doing this, the average value of the time series is subtracted to better visualize the fluctuations with respect to the average itself.

Finally, the significance of the power peaks in the spectra was confirmed through a randomization test^{32,33}. This approach was already used in the past for the significance estimation of oscillations in the solar atmosphere (see for instance³⁴). This technique relies on the random reshuffling of the time series in order to destroy temporal correlations. This process is performed several times, 1000 in our case, in order to assess the probability of the randomized time series to confirm the actual peaks of the spectrum that is assessed.

A series of state-of-the-art 3D MHD simulations were performed using Lare3d to demonstrate a possible formation mechanism for $m=1$ torsional Alfvén waves in the lower solar atmosphere. Lare3d is a Lagrangian remap code that solves the resistive MHD equations over a 3D staggered grid¹⁷.

A high-density, vertically stratified, divergent, flux tube is placed in the centre of the domain, representing the magnetic pore, and TAWs are then driven from the lower boundary, representing the observed photospheric surface.

The simulations performed are analogue to those presented in¹⁸ with the very important distinction that here the domain is the chromosphere rather than the corona. A non-zero plasma-beta of order unity is therefore used across the domain and chromospheric temperatures and densities are employed³⁵.

The simulations were executed over a grid with a resolution of 200 x 200 x 150. Two sets of simulations were run, one with dimensions of the domain of 8 Mm x 8 Mm x 3 Mm, and another one with 16 Mm x 16 Mm x 3 Mm to capture the torsional waves as part of the wider magnetic structure, with velocity perturbations exponentially damped in the upper 1 Mm of the domain to avoid wave reflection from the upper boundary.

The initial conditions prescribe a static equilibrium with a constant pressure and an axisymmetric exponentially divergent potential magnetic field. The magnetic field used is given by ³⁵, and is defined by the magnetic field in the radial and upward directions,

$$\begin{aligned} B_{0r} &= B_0 e^{-z/H} J_1(r/H), \\ B_{0z} &= B_0 e^{-z/H} J_0(r/H), \end{aligned}$$

where the characteristic value of the magnetic field $B_0 = 100$ G. The magnetic scale height $H = 10$ Mm and J_0 and J_1 are Bessel functions of the first kind and of zero and first order, respectively. This magnetic field configuration is visualised in Figure S4.

The initial density and temperature profiles are defined by,

$$\begin{aligned} \rho_0(r, z) &= \rho_{00} e^{-z/H} (2 - \tanh(r - R)), \\ T(r, z) &= \beta_0 \mu_m B_0^2 / 2 \mu_0 k_B \rho(r, z) \end{aligned}$$

where the characteristic density $\rho = 10^{-4}$ kg m⁻³, the tube radius $R = 2$ Mm, the reduced mass $\mu_m = 0.5$ assuming a fully ionised plasma. The initial density and temperature profiles are shown in Figure S5.

The gas pressure is constant, $P_0 = \beta_0 B_0^2 / 2 \mu_0$ and the plasma-beta is $\beta = \beta_0 (B_0^2 / B^2)$, where $\beta_0 = 1$. It can be shown that given a scale height of $H = 10$ Mm, β is never less than $\beta_0 / 2$ across the domain.

Alfvén waves are driven from the lower photospheric boundary of the domain throughout the simulations, the waves are driven across the photospheric boundary not just within the flux tube. The waves are driven in the transverse y -direction at three typical frequencies, corresponding to the frequencies observed, 0.45 mHz, 1.35 mHz and 2.25 mHz. The form of these perturbations are,

$$\begin{aligned} v_y &= a_0 f(t), \\ b_y &= B_y - a_0 f(t) \sqrt{\rho_0}, \\ f(t) &= \sin(\omega t) + \sin(3\omega t) + \sin(5\omega t), \end{aligned}$$

where v_y and b_y are the velocity and magnetic field perturbations, respectively, a_0 is the wave amplitude, $f(t)$ is the wave driving, B_y is the equilibrium magnetic field in the y -direction and the frequency is $\omega = 0.45$ mHz. The driving amplitude for the velocity is $a_0 = 0.223$ km/s and the driving amplitude for the magnetic field is 43.3 G.

By a simulation time of approximately 20 minutes, a typical computation reaches a quasi-equilibrium with wave driving. Simulations were each run for a total 112 minutes.

DAS: "The data that support the plots within this paper and other findings of this study are available from the corresponding author upon reasonable request."